Sensors and Materials, Vol. 37, No. 4 (2025) 1299–1310
MYU Tokyo

S & M 3988

Enantiomer Identification by Applying Electric Fields of Various Intensities to Microgaps Installed in a Gas Flow Channel

Manase Mizutani,[1,3] Naho Minowa,[1] Yong-Joon Choi,[1] Kazuhiro Takahashi,[1,2] Yoshihisa Suzuki,[3] Kazuaki Sawada,[1,2] and Toshihiko Noda[1,2*]

[1]Department of Electrical and Electronic Information Engineering, Toyohashi University of Technology, Toyohashi 441-8580, Japan
[2]Institute for Research on Next-generation Semiconductor and Sensing Science (IRES²), Toyohashi University of Technology, Toyohashi 441-8580, Japan
[3]Development Group, Sintokogio, Ltd., Toyokawa 442-8505, Japan

(Received August 7, 2024; accepted October 21, 2024)

Keywords: enantiomer identification, gas molecular sieving device, electrical field, discrimination, molecular geometric structure

Enantiomers are molecules whose structures are nonsuperimposable mirror images. Enantiomeric molecules have the same chemical and physical properties but may undergo different biological reactions. Therefore, distinguishing between enantiomers using most equipment is difficult. Thus far, enantiomers can only be identified using expensive analytical methods, such as gas chromatography, and active studies are underway on methods that distinguish between enantiomers using inexpensive gas sensors. Various weak enantiomeric gases are generated from living organisms and pharmaceuticals where asymmetric synthesis is performed. We can obtain detailed chemical information about living organisms and spaces by identifying these gases as different components. In this study, we focused on the charge bias caused by the differing geometric structures of enantiomers. We propose a grid that can apply electric fields of various strengths to a gas flow path. We believe that the electrical force acts on the charge held by the gas molecules, steepening the gas sensor output waveform and increasing the output value. We confirmed that molecules with enantiomeric relationships can be identified using grids. This research is expected to enable gas sensors to detect chemical components in more detailed classifications.

1. Introduction

Gas analysis is an essential analytical technology in the food, healthcare, and conservation fields. This study aimed to analyze aromas and putrid components in food, detect diseases such as diabetes by analyzing the concentration of volatile organic compounds (VOCs) in exhaled gas, and measure harmful volatile substances in the air and soil. Gas chromatography-mass spectrometry (GC-MS) is frequently used for the qualitative and quantitative analyses of complex vaporized components at low concentrations.(1,2) However, a GC-MS system is

*Corresponding author: e-mail: noda.toshihiko.zk@tut.jp
https://doi.org/10.18494/SAM5304

ISSN 0914-4935
https://myukk.org/

expensive and is generally used as a stationary device; therefore, it has the disadvantage of poor portability. In contrast, gas sensors are not as accurate for detecting gas components as the GC-MS system, but they are small, inexpensive, and easy to use for detecting gas components. Various detection methods exist for gas sensors, such as semiconductor,[3–6] electrochemical,[7,8] quartz crystal micro-balance (QCM),[9–12] and membrane-type surface stress (MSS)[13,14] gas sensors. These are used, for instance, to measure the components of automobile exhaust gas or alcohol in human breath. Gas sensors are small and can be manufactured at a low cost. Therefore, new gas sensing systems that use multiple gas sensing methods and incorporate machine learning to identify and quantify gas molecules are being developed. However, the number and types of gas molecules present in air are enormous. Therefore, it may be difficult to use a gas sensor unless the identity of the gas is known, and collecting data based on various properties, such as the composition and polarity of the gas components, is necessary.

Although enantiomers generally exhibit the same chemical and physical properties, their physiological activities may differ. To humans, (+)-limonene has a similar smell to lemons and (−)-limonene has a similar smell to oranges.[15] Gaseous enantiomers play important roles in various chemical and biological processes, including food,[16] plant physiology,[17,18] nerve drug production,[19] and essential oils.[20] Methods for analyzing enantiomers using GC-MS include measuring the optical purity, that is, *ee* using a special chiral column. In addition, by installing an isotopic ratio mass spectrometer downstream of the GC device, ionized gas molecules are separated using magnetic force to identify and quantify enantiomers.[21,22]

When a gas sensor is used in a typical way to discriminate between enantiomers, the waveforms of the gas sensor outputs are similar. Furthermore, the output value may vary depending on measurement experiment settings. In contrast, because the sensitivity of gas sensors varies depending on environmental conditions, such as humidity, their output value does not only reflect the target gas. Therefore, to realize enantiomer discrimination using a gas sensor, additional elements that vary the gas sensor output depending on the target gas and measurement environment are required. Several methods for identifying enantiomers using gas sensors have recently been reported. [23–25] For instance, Maity *et al.* stated that enantiomers can be detected using the chiral-induced spin selectivity effect in which electrons in a molecule are aligned in a specific direction by an electric or magnetic field.[24] They designed a device using a molecular spin-sensitive antenna (MSSA) receptor and identified (+)- and (−)-butanol on the basis of the difference in electrical signal. In their proposed device, the MSSA was coated on conductive graphite, and organic ligands were connected to the MSSA in a manner perpendicular to the graphite surface. A change in the resistance of graphite occurs only when the molecule adsorbed on the organic ligand is polarized, and the enantiomers are discriminated by an increase or decrease in resistance. In addition, Okur *et al.* proposed a QCM-type gas sensor in which a film coated with different metal–organic frameworks (MOFs) was attached to the surface of a crystal, and the functions were determined using five pairs of gaseous enantiomers.[25] MOFs comprise metal ions and organic ligands. Some organic ligands have enantiomeric relationships and may exhibit different adsorption properties for the enantiomers of gas molecules.[25] However, in previous studies, the sample concentration was on the order of ppm, and the measurement time was limited because of the adsorption phenomenon. Using the

grid introduced below, we can perform long-term measurements and clearly obtain the waveforms of samples with concentrations on the order of ppb.

The grid can change the physical or chemical properties of different gases; thus, a simple sensor system can identify the various gases. We previously proposed slit-structured elements (grids) that sieve gas molecules before they reach the gas sensor (Fig. 1).[26,27] A grid is a device that changes the output of a gas sensor by filtering gas molecules on the basis of their properties. Thus far, we have verified the sieving of gas molecules by changing the grid spacing, applying an electric field around the grid, and using a metal with a catalytic effect, such as platinum, in the grid. First, we measured the gas sensor output for the same concentration of ammonia with and without the grid installed along the gas flow path. Subsequently, the gas sensor output decreased owing to the installation of the grid. Furthermore, when the grid spacing was changed to 10 and 7.5 μm, the output of the 7.5 μm gas sensor became smaller.[26] Regarding this result, we believe that narrowing the grid pitch makes it difficult for most of the gas to enter the gaps in the grid, impeding the permeation of the gas toward the gas sensor. Second, an electric field was applied to the grid to allow the gas to pass through, and the output of the gas sensor for ammonia improved as the applied voltage increased. In contrast, the gas sensor output did not change for ethanol and decreased for acetic acid as the applied voltage increased.[26] Finally, when the grid material was Pt, the gas sensor output for ammonia was measured by heating it with electricity. The output can change depending on the current value because of the decomposition of ammonia owing to the catalytic effect of Pt.

Among these cases, applying a voltage to the grid (Fig. 2) allows for differences in applied voltage dependence to be used to identify the gas. This implies that the grid does not need to be replaced to change its dimensions or target gas, meaning measurements can be performed continuously. In this study, we focused on the charge bias caused by the differing geometric structures of enantiomers. We believe that by creating an electric field and increasing its strength, the Coulomb force acts on the charge held by the gas molecules, steepening the gas sensor output waveform and increasing the output value. Consequently, molecules with enantiomeric relationships can be identified.

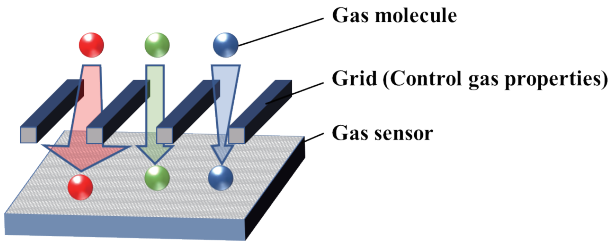

Fig. 1. (Color online) Schematic of a grid installed in front of a gas sensor.

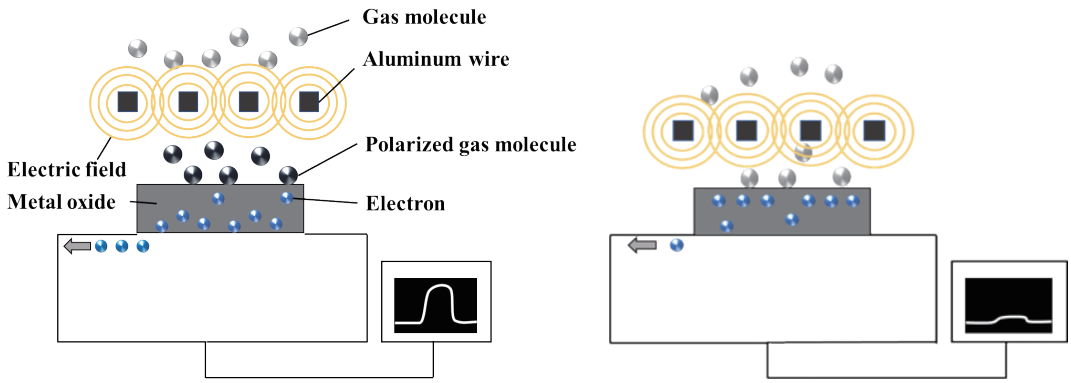

Fig. 2. (Color online) Scenario where gas molecules reach the detection area of a semiconductor-type gas sensor. (a) Molecules affected by the electric field of the grid reach the gas sensor. (b) Molecules reach the gas sensor without being affected by the electric field of the grid.

2. Materials and Methods

2.1 Grid design

A grid was formed on a 10 × 10 mm^2 silicon substrate. The silicon substate has 6 × 6 through holes with dimensions of 300 × 300 μm^2 and aluminum wires are laid out at 15 μm intervals on the silicon substate. The Al wires were wired such that positive and negative voltages can be applied alternately, and when a voltage was applied, an electric field was generated between the Al wires. Therefore, when gas passes through a through hole, it passes through the electric field (Fig. 3). The electric field strength was varied by varying the applied voltage. Figure 3 shows an enlarged view of one of the 36 through holes.

2.2 Grid fabrication

A 2 inch silicon wafer was used as the starting material. The fabrication of the grid was based on the MEMS process, and the steps were as follows (Fig. 4).

(a) A 2 inch silicon wafer was thermally oxidized to form a 400-nm-thick oxide film.
(b) The oxide film (front side) of the through hole portion was removed.
(c) An 800-nm-thick Al film was then sputtered and patterned onto the surface.
(d) The oxide film in the thorough hole area on the rear side was removed.
(e) The silicon wafer was deep-etched from the back side by reactive ion etching.
(f) Through holes were formed by XeF_2 isotropic etching.

Finally, the fabricated grid chips were cut from the silicon wafer by laser dicing. The grid after fabrication is shown in Fig. 5.

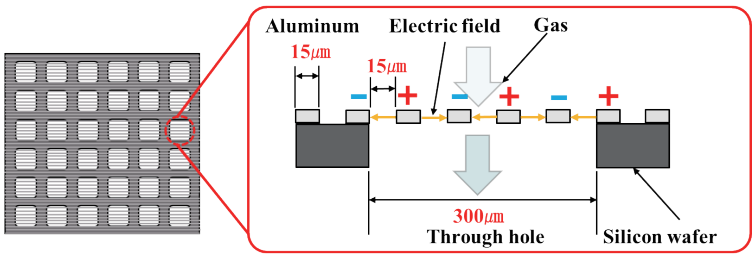

Fig. 3. (Color online) Cross-sectional diagram of a through hole, silicon wafer, and Al wire.

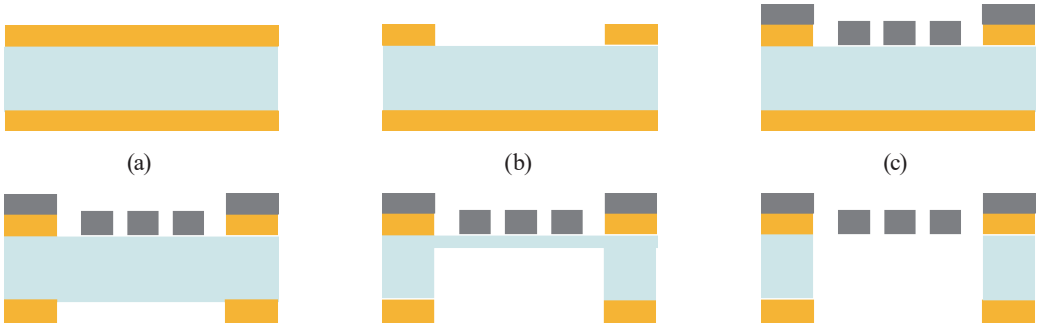

Fig. 4. (Color online) Cross-sectional diagram showing the grid fabrication process. (a) Thermal oxidation. (b) SiO_2 etching (front side). (c) Al patterning. (d) SiO_2 etching (back side). (e) Deep RIE. (f) XeF_2 etching.

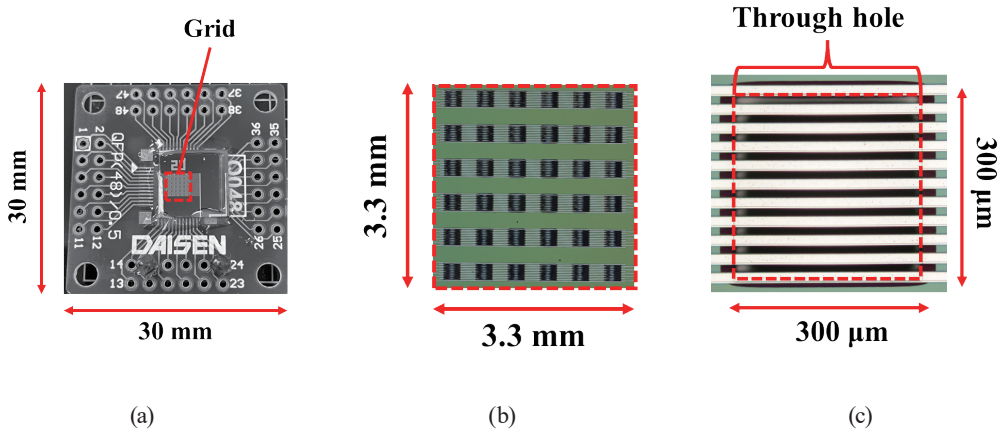

Fig. 5. (Color online) Photograph of the fabricated grid. (a) PCB with fixed grid. (b) Through hole arrangement. (c) Microscopic photo of one through hole.

2.3. Characterization procedure

First, the printed circuit board (PCB) with the grid fixed was placed on top of the jig that will fix the gas sensor. In this experiment, we used a semiconductor gas sensor module [CCS-811 (ams-OSRAM AG)], which detects gases through changes in conductivity. The concentration output of the gas sensor was expressed as equivalent total volatile organic compound (eTVOC).

CCS811 is a metal oxide gas sensor with a microcontroller unit (MCU) that includes an analog-to-digital converter and an I²C interface. eTVOC is calculated using an algorithm in the MCU from the raw measurement values from the gas sensor. In addition, the values range from 0 to 32768, and the units are expressed in ppb.[28] However, the method of analyzing VOCs in indoor air is specified in ISO16000-5. The general method is to sample VOCs using synthetic adsorbent tubes, such as Tenax tubes, and to analyze the VOCs that have been thermally desorbed from the adsorbent using GC-MS.[29] Therefore, directly citing the detection results of gas sensors is not a general analytical method.

In a semiconductor gas sensor, when the surrounding air is filled with inert N_2 gas, the electrons inside the detection section area are attracted to the surface oxide film and the output is 0. When gas molecules reach the detection section, electrons are supplied from the molecules to the oxide film via a redox reaction, and the electrons inside the detection section are released. The number of electrons emitted at this time is the output.

The unit also has a φ6 hole for gas to pass through that must be aligned on the PCB (Fig. 6). A pump was placed downstream of the jig and a gas bag was placed upstream. They were connected with a urethane tube with an inner diameter of 6 mm (Fig. 7). The gaps in the gas flow path were filled with adhesive rubber to prevent gas leakage.

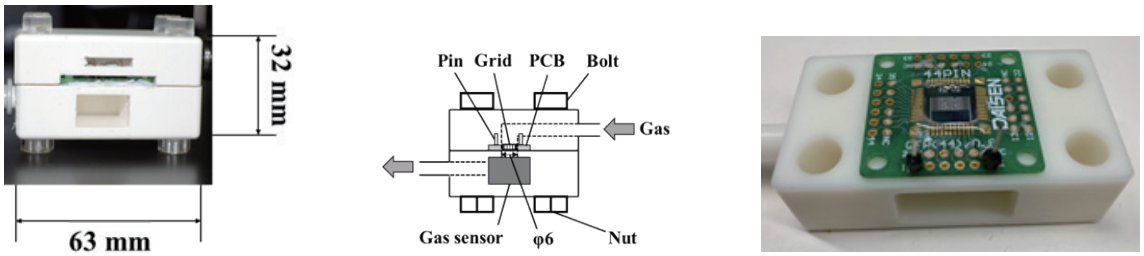

(a) (b) (c)

Fig. 6. (Color online) (a) Photograph of the designed jig. (b) Cross-sectional diagram of the jig. (c) Attaching the grid to the jig.

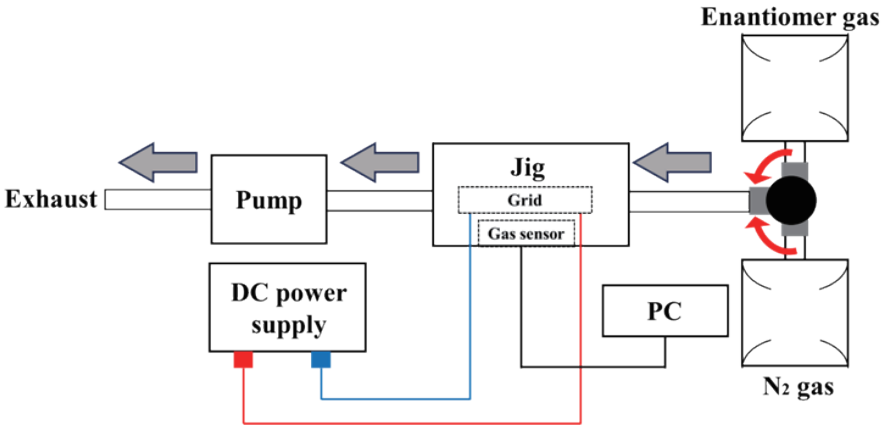

Fig. 7. (Color online) Block diagram of the experimental system.

We selected three pairs of enantiomers as targets, namely, (+)- and (−)-α-pinene, (+)- and (−)-limonene, and (+)- and (−)-carvone. Studies on sensing (+)- and (−)-α-pinene as an indicator of plant health are underway.[17] Additionally, (+)-limonene has a similar smell to oranges, whereas (−)-limonene has a similar smell to lemons. (+)-carvone has a similar smell to caraway seeds, whereas (−)-carvone has a similar smell to spearmint.[30] Figure 8 shows the structures of the enantiomers. α-Pinene, limonene, and carvone all have a six-membered ring with one double bond. α-Pinene and limonene belong to the lipophilic terpene group. In addition to the six-membered ring, α-pinene has three methyl groups (–CH3) and a four-membered ring, and limonene has one –CH3 and one –C=CH2–CH3 group. In comparison with α-pinene, limonene has a larger functional group with a double bond outside the six-membered ring; thus, it is prone to collisions with surrounding radicals and ions. Limonene is more susceptible to the effects of

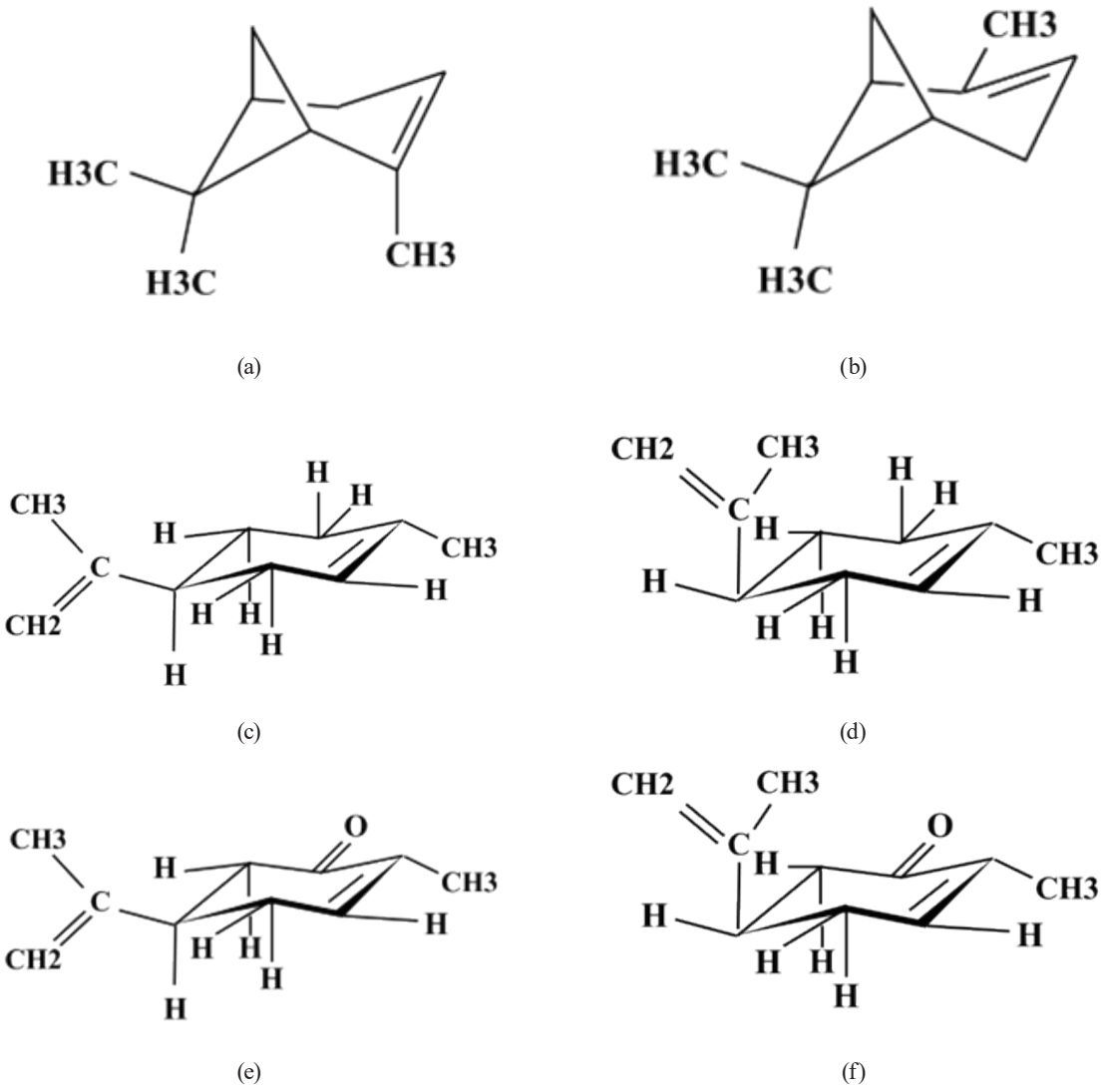

Fig. 8. Structures of α-pinene, limonene, and carvone. (a) (+)-α-pinene, (b) (−)-α-pinene, (c) (+)-limonene, (d) (−)-limonene, (e) (+)-carvone, and (f) (−)-carvone.

an electric field because the electric field produces more radicals and ions. Carvone has an additional carbonyl group in the limonene structure. The enantiomer gas was produced using a Permeator PD-1B (GASTEC Corporation). A total of 2 mL of the liquid sample was placed in a diffusion tube (D-10, GASTEC Corporation). Next, the diffusion tube was placed in the permeator at 40 ℃. The flow rate of N_2 for dilution was set to 0.5 L/min. After exhausting the gas for approximately 30 min, the sample gas was introduced into a flek sampler (Omi Odor Air Service Co., Ltd.) with a capacity of 20 L while maintaining a flow rate of 0.5 L/min. The gas produced from (+)- and (−)-α-pinene was confirmed to have a concentration of 300 ppb using a detection tube (121SP, GASTEC Corporation).

The gas sensor was exposed to N_2 gas for 100 s, to the enantiomer gas for 100 s, and again to N_2 gas for 100 s. The N_2 gas did not affect the gas sensor output. The gas sensor output was sampled every 5 s. The voltages applied to the grid were in the following order: 0, 10, 20, 30, 40, 50, 60, 70, and 80 V. Each was repeated thrice and the average value was reported.

3. Results

Figure 9 shows time series data of the gas sensor output for the enantiomers of α-pinene, limonene, and carvone when voltages of various strengths were applied to the grid. When the enantiomers were each made to respond to the sensor alone, no difference in output was observed. The vertical axis was normalized such that the saturation value was 1 when 0 V was applied. When a voltage was applied to the grid, the gas sensor output values for (+)-α-pinene and (−)-limonene increased significantly compared with their respective enantiomers. Regarding carvone, the gas sensor output gradually increased as the applied voltage increased for both enantiomers. Among them, (−)-carvone exhibited a relatively large increase.

Figure 10 shows the dependence of the saturation value of the normalized eTVOC on the applied voltage. The saturation value of (+)-α-pinene changed significantly at 10 V, increasing by approximately 1.5 times, and gradually decreased as the applied voltage was increased from 20 to 80 V. In contrast, the output of (-)-α-pinene did not change significantly even when voltage was applied. Therefore, when a voltage in the range from 10 to 30 V was applied to α-pinene, the difference in gas sensor output between the enantiomers increased and discrimination could occur. For (−)-limonene, the saturation value changed significantly at an applied voltage of 20 V, increasing by approximately 2.7 times, and the saturation value gradually decreased at an applied voltage in the range of 30–80 V. In contrast, the output of (+)-limonene did not change significantly even when voltage was applied. Therefore, when a voltage of 20 V or more was applied to limonene, the difference in gas sensor output between the enantiomers increased, making it possible to identify the enantiomers. The saturation value of (−)-carvone gradually increased as the applied voltage value increased. For (+)-carvone, the saturation value gradually increased up to an applied voltage of 50 V, but gradually decreased for an applied voltage in the range of 60–80 V. No notable difference existed in the response of (+)- and (−)-carvones owing to voltage application, but the gas sensor output increased to a greater extent for (−)-carvone than for (+)-carvone. From this perspective, we can distinguish between carvone enantiomers.

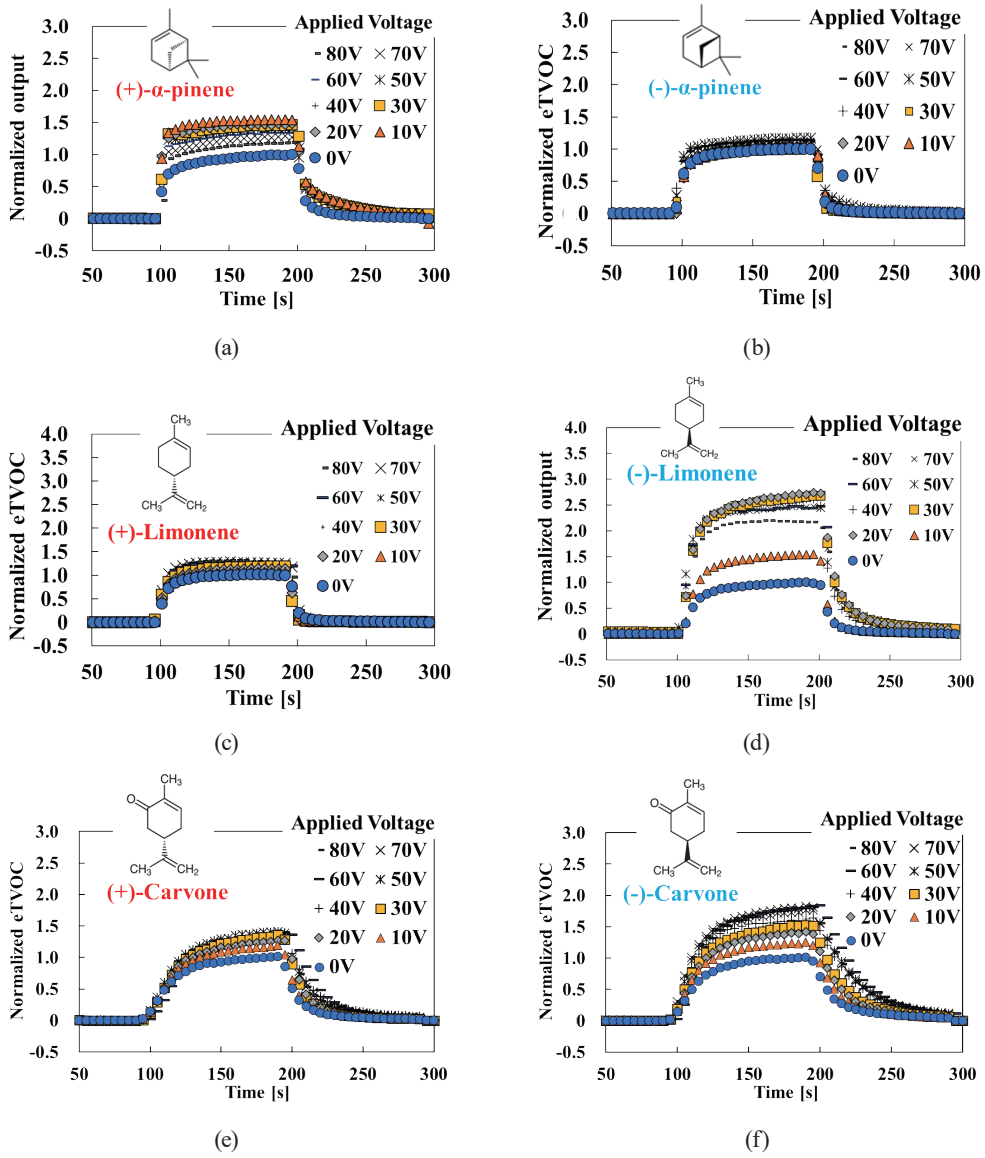

Fig. 9. (Color online) Time series data of gas sensor output for various chiral molecules.

4. Discussion

On the basis of the differences in their chemical structures (Fig. 8), enantiomers should respond differently to an applied electric field. (+)-α-pinene, (−)-limonene, and (−)-carvone, which are more strongly affected by electric fields, have functional groups that bond perpendicularly to the six-membered ring. In components in which the sensor output increases because of an external electric field, the functional groups formed on the outside of the six-membered ring may electrically repel other atoms. Therefore, the molecules become less stable, and the movement of electrons becomes active, which is considered to cause the increase in gas sensor output. In contrast, the other enantiomers did not strongly repel other atoms, even when

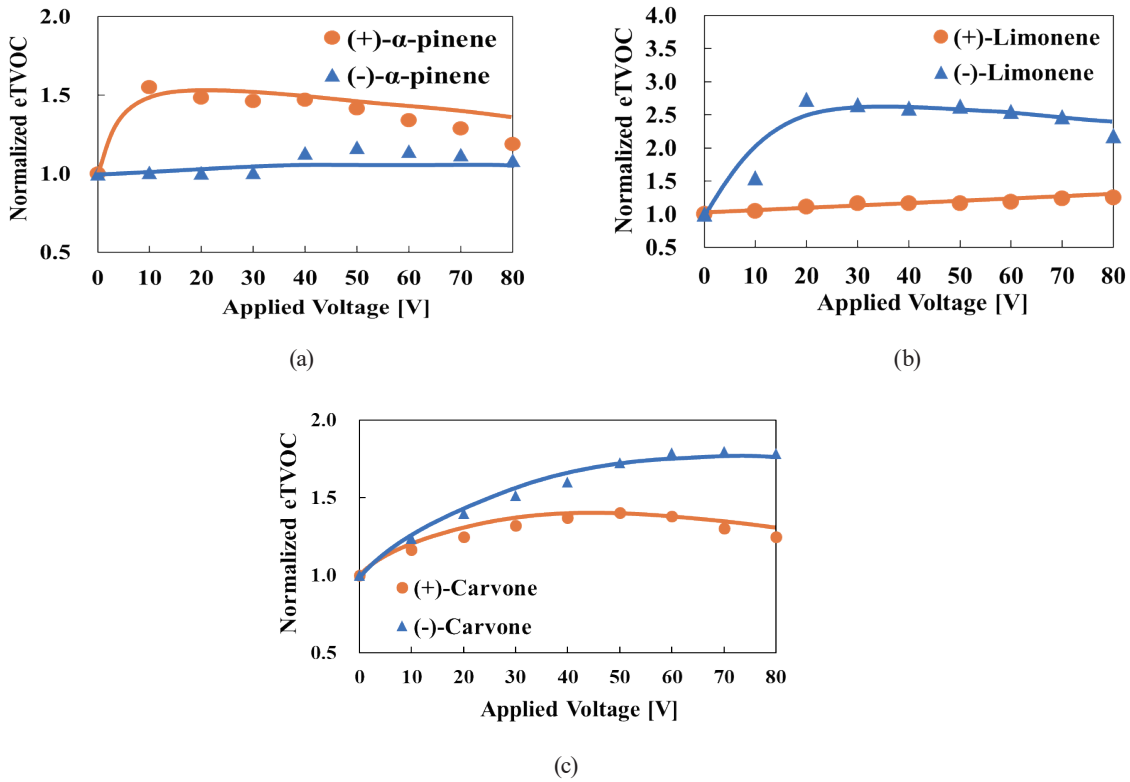

Fig. 10. (Color online) Applied voltage dependence of the saturation value of normalized eTVOC.

exposed to an external electric field, because the functional group was bonded in a stable conformation. In a semiconductor gas sensor, when molecules reach the detection section, a redox reaction occurs, and electrons are released from the oxide film, increasing the output.[3–6,27] The more active the movement of electrons in the arriving molecule, that is, the higher its energy level, the more likely it is that a redox reaction will occur. The energy level of molecules affected by an electric field differs depending on their molecular structure, resulting in differences in gas sensor output when it reaches the detection section. Furthermore, when the concentration of molecules affected by the electric field around the gas sensor reached a peak, the gas sensor output was considered saturated. Because peak values are present in the plots, we consider that optimizing the applied voltage can improve the ability of the gas sensor to identify gas molecules.

5. Conclusions

In this study, we focused on the bias in molecular charge caused by the geometric structure of enantiomers. Such effects were confirmed by applying electric fields of various strengths to a grid installed along the gas flow path.

For α-pinene, when the applied voltage is in the range of 10–30 V, and for limonene, when the applied voltage is 30 V or more, the difference in gas sensor output between enantiomers increases, making it possible to distinguish between their enantiomers. Carvone exhibits no

significant difference in response between (+)- and (−)-carvones when a voltage is applied. However, because the gas sensor output of (−)-carvone is much higher than that of (+)-carvone, we can distinguish between enantiomers.

In a semiconductor gas sensor, when molecules reach the detection part, a redox reaction occurs and electrons are released from the oxide film, increasing the output. Enantiomers have different gas sensor outputs after being affected by an electric field owing to differences in their energy levels, and they can be identified. The results of the procedure developed herein are expected to be applicable to isomers other than enantiomers, provided that the components have different charge biases (dipole moments).

In this study, a single component was used. In future studies, we will use the developed gas sensor to analyze mixtures. However, there is a high possibility that it is difficult to analyze a mixture of components having similar applied voltage values when the gas sensor output value is maximized.

Acknowledgments

This work was supported in part by the MEXT Initiative to Establish the NeXt-Generation Novel Integrated Circuits Center S (X-NICS) (Grant Number: JPJ011438), JST OPERA Program (Grant Number: JPMJOP1834), and JSPS KAKENHI, Japan (Grant Number: JP21K18718).

References

1 D. S. Yang, R. L. Shewfelt, K.-S. Lee, and S. J. Kays: J. Agric. Food Chem. **56** (2008) 2780. https://doi.org/10.1021/jf072685t
2 S. Z. Hussain and K. Maqbool: Int. J. Curr. Sci. **13** (2014) 116.
3 D. Rüffer, F. F. Hoehne, and J. J. Bühler: Sensors **18** (2018) 1052. https://doi.org/10.3390/s18041052
4 M. V. Nikolic, V. Milovanovic, Z. Z. Vasiljevic, and Z. Stamenkovic: Sensors **20** (2020) 6694. https://doi.org/10.3390/s20226694
5 S. P. Lee: Sensors **17** (2017) 683. https://doi.org/10.3390/s17040683
6 M. Dadkhah and J.-M. Tulliani: Sensors **22** (2022) 4669. https://doi.org/10.3390/s22134669
7 A. G. MacDiarmid: Angew. Chem. Int. Ed. **40** (2001) 2581. https://doi.org/10.1002/1521-3773(20010716)40:14<2581::AID-ANIE2581>3.0.CO;2-2
8 J. Baranwal, B. Barse, G. Gatto, G. Broncova, and A. Kumar: Chemosensors **10** (2022) 363. https://doi.org/10.3390/chemosensors10090363
9 P. Si, J. Mortensen, A. Komolov, J. Denborg, and P. J. Møller: Anal. Chim. Acta **597** (2007) 223. https://doi.org/10.1016/j.aca.2007.06.050
10 K. Nakamura, T. Nakamoto, and T. Moriizumi: Sens. Actuators, B **69** (2000) 295. https://doi.org/10.1016/S0925-4005(00)00510-4
11 S. I. Boyadjiev and M. M. Rassovska: ELECTRONICS' 2007.
12 F. Pascal-Delannoy, B. Sorli, and A. Boyer: Sens. Actuators **84** (2000) 285. https://doi.org/10.1016/S0924-4247(00)00391-5
13 H. T. Ngo, K. Minami, G. Imamura, K. Shiba, and G. Yoshikawa: Sensors **18** (2018) 1640. https://doi.org/10.3390%2Fs18051640
14 F. Loizeau, T. Akiyama, S. Gautsch, P. Vettiger, G. Yoshikawa, and N. de Rooij: Procedia Eng. **47** (2012) 1085. https://doi.org/10.1016/j.proeng.2012.09.339
15 L. Kvittingen, B. J. Sjursnes, and R. Schmid: J. Chem. Educ. **98** (2021) 3600. https://doi.org/10.1021/acs.jchemed.1c00363
16 A. Vergara, S. Vembu, T. Ayhan, M. A. Ryan, M. L. Homer, and R. Huerta: Sens. Actuators, B **166–167** (2012) 320. https://doi.org/10.1016/j.snb.2012.01.074
17 J. Byron, J. Kreuzwieser, G. Purser, J. van Haren, S. N. Ladd, L. K. Meredith, C. Werner, and J. Williams: Nature **609** (2022) 307. https://doi.org/10.21203/rs.3.rs-770148/v1

18 J. Bohlmann, C. L. Steele, and R. Croteau: J. Biol. Chem. **272** (1997) 21784. https://doi.org/10.1074/jbc.272.35.21784
19 D. P. D. Sousa, F. F. D. Fariasnóbrega, and R. N. D. Almeida: Chirality **19** (2007) 264. https://doi.org/10.1002/chir.20379
20 G. Frensch, R. Labes, C. L. Wosch, L. dos S. Munaretto, K. S. Salomé, P. G. Guerrero Jr., and F. A. Marques: Tetrahedron Lett. **57** (2016) 420. https://doi.org/10.1016/j.tetlet.2015.12.042
21 D. Sciarrone, L. Schipilliti, C. Ragonese, P. Q. Tranchida, P. Dugo, G. Dugo, and L. Mondello: J. Chromatogr. A **1217** (2010) 1101. https://doi.org/10.1016/j.chroma.2009.09.080
22 L. Cucinotta, G. D. Grazia, P. Donato, M. Mondello, D. Sciarrone, and L. Mondello: J. Chromatogr. A **1710** (2023) 464409. https://doi.org/10.1016/j.chroma.2023.464409
23 R. Naaman and D. H. Waldeck: Annu. Rev. Phys. Chem. **66** (2015) 263. https://doi.org/10.1146/annurev-physchem-040214-121554
24 A. Maity, Y. Hershkovitz-Pollak, R. Gupta, W. Wu, and H. Haick: Adv. Mater. **35** (2023) 2209125.
25 S. Okur, P. Qin, A. Chandresh, C. Li, Z. Zhang, U. Lemmer, and L. Heinke: Angew. Chem. Int. Ed. **60** (2021) 3566. https://doi.org/10.1002/anie.202013227
26 R. Wada, N. Minowa, T. Wada, M. Mizutani, Y. Suzuki, Y.-J. Choi, K. Takahashi, K. Sawada, and T. Noda: IEEE Sensors (2021) B1L-01.
27 N. Minowa, M. Mizutani, Y. Suzuki, Y.-J. Choi, K. Takahashi, K. Sawada, and T. Noda: Transducers (2023) W4P.030.
28 ams-OSRAM AG Datasheet CCS811: https://cdn.sparkfun.com/assets/2/c/c/6/5/CN04-2019_attachment_CCS811_Datasheet_v1-06.pdf (accessed on January 11, 2024).
29 ISO 16000-5 Indoor air: Part 5: Sampling strategy for volatile organic compounds (VOCs).
30 K. D. Klika: ISRN Organic Chemistry **2013** (2013) 515810. https://doi.org/10.1155/2013/515810